



# Laboratory measurements of seismo-magnetic conversions in fluid-filled Fontainebleau sand

**Clarisse Bordes**, LGIT Université Joseph Fourier, Grenoble (France)

**Laurence Jouniaux**, EOST Université Louis Pasteur, Strasbourg (France)

**Michel Dietrich**, LGIT Université Joseph Fourier, Grenoble (France)

**Jean-Pierre Pozzi**, Ecole Normale Supérieure, Paris (France)

**Stéphane Garambois**, LIRIGM Université Joseph Fourier, Grenoble (France)

January 2006

## Abstract

Seismic wave propagation in fluid-filled porous materials induces electromagnetic effects due to small relative pore-fluid motions. In order to detect the seismo-magnetic couplings theoretically predicted by Pride (Phys. Rev. B, 50:15678-15695, 1994), we have designed a small-scale experiment in a low-noise underground laboratory which presents exceptional electromagnetic shielding conditions. Our experiment included accelerometers, electric dipoles and induction magnetometers to characterize the seismo-electromagnetic propagation phenomena. To assess the electrokinetic origin of the measured electric and magnetic fields, we compared records obtained in dry and fluid-filled sand. Extra care has been taken to ensure the mechanical decoupling between the sand column and the magnetometers to avoid spurious vibrations of the magnetometers and misinterpretations of the recorded signals. Our results show that seismo-electric and seismo-magnetic signals are associated with different wave propagation modes, thus emphasizing the electrokinetic origin of these effects.

# 1 Introduction

Observations of transient electromagnetic phenomena accompanying the seismic wave propagation in fluid filled porous media date back at least to the work of *Ivanov* (1940). *Frenkel* (1944) gave the first quantitative explanations of these phenomena in term of electrokinetic effects at the pore scale until *Pride* (1994) developed a complete theory which prompted further studies.

Early and pioneering work by *Martner and Sparks* (1959) and *Thompson and Gist* (1993) and more recent studies by *Takeuchi et al.* (1997), *Mikhailov et al.* (2000), and *Garambois and Dietrich* (2001) have concentrated on field measurements. Laboratory measurements were notably performed by *Zhu et al.* (2000), and *Zhu and Toksöz* (2005) whereas numerical simulations were performed by *Haartsen and Pride* (1997), *Garambois and Dietrich* (2002) and *White* (2005).

Two kinds of seismo-electromagnetic effects are to be distinguished. The dominant contribution we are addressing in this paper corresponds to electrical and magnetic coseismic fields accompanying the body and surface waves. The second kind is generated at physico-chemical properties contrasts and consists of independantly propagating electromagnetic waves.

Seismo-electromagnetic studies have generally concentrated on the measurements of electrical fields as they require only a simple instrumentation. The investigation of seismo-magnetic fields has received much less attention mainly because of the high level of electromagnetic noise affecting the magnetic measurements. In order to minimize these disturbances, we have designed a laboratory experiment within the ultra-shielded chamber of the LSBB low-noise laboratory located in Rustrel, southern France.

This paper describes the experimental apparatus as well as the first results (seismic, electric and magnetic responses) measured in homogeneous Fontainebleau sand. We show that seismo-magnetic conversions are weak but nevertheless measurable. Moreover, the different apparent velocities characterizing the seismo-electric and seismo-magnetic events emphasize that they are associated to different propagation modes.

## 2 Experimental apparatus

The LSBB facilities were originally an underground launching center for the ground-based component of the French strategic nuclear defense. A characterization of the electromagnetic shielding, performed by *Gaffet et al.* (2003), using a SQUID magnetometer showed that the noise level is below  $2 \text{ fT}/\sqrt{\text{Hz}}$  above 10 Hz.

Our experimental apparatus was located within the shielded chamber and consisted of a porous sample, a seismic source and sensors. The whole experiment including the triggering of the mechanical source and the data acquisition was remotely controlled from outside the chamber to suppress electromagnetic perturbations from the instruments. All measurements were performed with a 24 bit seismic recorder (Geometrics StrataVisor NZ) using a  $21 \mu\text{s}$  time sampling rate.

### 2.1 Seismo-electric and seismo-magnetic measurements.

Our experiments were performed with two 1 m high and 8 cm diameter vertical Plexiglas columns filled with Fontainebleau sand (figure 1). This sand contains 99 % of silica with grain size smaller than  $300 \mu\text{m}$ . The measured permeability of the sand is  $5.8 \cdot 10^{-12} \text{ m}^2$  and its bulk density  $1.7727 \cdot 10^3 \text{ kg/m}^3$ , its electrical resistivity is  $22 \text{ k}\Omega\cdot\text{m}$ , and the water conductivity is  $3.1 \text{ mS/m}$  with a pH of 6.55 at  $20.5 \text{ }^\circ\text{C}$ . The sand was compacted by vibrating the column during filling in order to minimize the pore space and high frequency seismic wave attenuation. The seismic velocities in the partially saturated sand can be estimated by considering reasonable values of the bulk frame modulus ( $1.3 \cdot 10^9 \text{ Pa}$ ) and shear frame modulus ( $1.4 \cdot 10^9 \text{ Pa}$ ). By using these values in relations given by *Pride and Haartsen* (1996) the computed  $P$  and  $S$  wave velocities are respectively equal to 1300 and 870 m/s.

The first column was equipped with ten unpolarizable electrodes (silver rods and porous ceramics) spaced 10 cm apart along the column generatrix. These electrodes were previously used for streaming potential measurements and are described in *Guichet et al.* (2003). We chose to use a common reference

electrode at the bottom end of the column. Electrical measurements (mV) are normalized by the dipole spacing to provide equivalent electrical field (mV/m). This column was also equipped with four accelerometers fixed on the outer Plexyglas surface.

The second column was especially used for the seismo-magnetic measurements which are much more sensitive to external perturbations. Even if it is reduced within the capsule, we have to take into account the constant magnetic field. Indeed, the motions of the magnetometers may generate induction effects resembling coseismic effects and masking the seismo-magnetic signals of interest. We designed a suspension system for the seismic source on the capsule ceiling to avoid the transmission of mechanical vibrations to the magnetometers. Moreover, the magnetometers were fixed on a separate stand, and were isolated from ground vibrations by a soundproofing material. However, test accelerometers fixed on the magnetometers showed that residual vibrations arrive 5 ms after the seismic impacts. These disturbances appear later than the seismic and seismo-electromagnetic signals but are nevertheless in the time window considered (-1 ms to 10 ms).

The upper magnetometer can be moved into seven locations which exactly correspond to the electrode positions in term of source-receiver spacing (figure 1). The two missing locations correspond to the column fastening. The lower magnetometer is used as a common reference similarly to the electrical measurements, in order to cancel synchronous disturbances such as accelerometer radiation.

The theory of *Pride* (1994) stipulates that in a homogeneous infinite fluid-saturated porous medium, the coseismic seismo-electric fields are traveling with longitudinal  $P$ -waves whereas seismo-magnetic signals are associated with transverse  $S$ -waves. For porous cylinders, we have to consider global and local deformations and their propagation in the structure. The maximum displacements due to a vertical seismic excitation are associated with extensional modes. In the elastic case, the extensional wave velocity is derived from Young's modulus  $E$  and total density  $\rho$  ( $V_{ext} = \sqrt{E/\rho} = 1300$  m/s) and is close to the  $P$ -wave velocity. Thus, waves propagating at a velocity of 1300 m/s will be associ-

ated with  $P$  and extensional modes whereas waves traveling at approximately 870 m/s will be associated with  $S$  waves. We used an induction magnetometer whose sensitivity on the radial and tangent components is quite constant in the 100 Hz to 2 kHz range.

## 2.2 EM noise free pneumatic seismic source

Piezoelectric seismic sources are often used for seismo-electric laboratory measurements (Ageeva *et al.*, 1999; Zhu *et al.*, 2000). These sources, however, are not well suited for seismo-magnetic measurements because of their intrinsic electromagnetic radiation. In order to minimize the magnetic perturbations generated by the seismic excitation, we built a pneumatic system (figure 2) capable of generating a large number of impacts within a few minutes. This feature allows us to improve our data by stacking successive recordings.

An accelerometer placed on the granite cylinder records the source time function. The latter is rather impulsive and has a broad-band spectrum ranging from 100 Hz to 10 kHz. To compare the records obtained from different shots, the signals are all normalized with respect to a reference excitation of  $1000 \text{ m/s}^2$  ( $\simeq 100 \text{ g}$ ).

## 3 Results

Since our objective is to demonstrate the existence of seismo-electromagnetic fields due to fluid-grain interactions, we compared the electric, magnetic and seismic responses measured in dry and fluid-filled homogeneous sand. The signals presented in figure 3 were obtained by stacking 10 accelerometric, 10 seismo-electric, and 100 seismo-magnetic records. The panels displayed in figure 3 respectively present the seismic (top), seismo-electric (middle) and seismo-magnetic (bottom) responses obtained in dry sand (left) and fluid-filled sand (right). The spectra of seismic and electric signals were computed from the complete time sequences whereas the spectra of the magnetic signals were limited to the (-1 ms to 4 ms) time window.

### 3.1 Homogeneous dry sand

The first arrivals of the accelerometric signals recorded in dry sand show an apparent velocity of  $1201 \pm 85$  m/s in the 700 Hz to 3 kHz frequency range (figure 3a). However, panels 3b and 3c show that the seismic wave propagation in homogeneous dry sand does not produce any coherent electromagnetic fields. The electrodes only pick up instrumental noise with amplitudes lower than 0.4 mV/m for an impact of  $1000 \text{ m/s}^2$  (figure 3b). Nevertheless, the trace located nearest to the source shows a weak signal ( $1.4 \text{ mV/m}/1000 \text{ m/s}^2$ ) probably associated with a piezoelectric effect due to the excitation of quartz grains in perfectly resistive conditions. Similarly, the magnetic signals (figure 3c) display low frequency noise caused by internal electronic disturbances of the magnetometers.

### 3.2 Fluid-filled homogeneous sand

The seismic records presented in figure 3d are slightly modified by the presence of water. The lower frequency content of the signals seen in figure 3d, as compared to figure 3a, can be explained by the fact that in *Biot* (1956) theory, high frequencies are strongly attenuated due to fluid flow at the pore scale. The similarity of the apparent velocities of the first seismic arrivals in dry and saturated conditions is consistent with a fluid saturation lower than 80 % according to the *Knight and Nolen-Hoeksema* (1990) measurements in rocks.

When the sand is filled with water, electric and magnetic fields records are strongly modified. In particular, we observe that the amplitudes of the seismo-electric signals generated in the fluid-filled sand ( $10 \text{ mV/m}/1000 \text{ m/s}^2$ , figure 3e) are 30 times larger than the electrical noise level in dry sand. The contributions of seismo-electric conversions are visible in both the time section and corresponding amplitude spectrum in the 200 Hz to 2 kHz range.

By contrast, the maximum amplitudes of the seismo-magnetic signals are only 3 times as high as in dry sand. Consequently, seismo-magnetic signals are barely visible in the associated amplitude spectrum (figure 3f). However, there is clear evidence of coherent arrivals in the time section. The presence of these events indicates some weak but non-zero seismo-magnetic coupling.

The differences between the apparent velocities of the first arrivals of the seismo-electric ( $1260 \pm 124 \text{ m.s}^{-1}$ ) and seismo-magnetic signals ( $791 \pm 80 \text{ m.s}^{-1}$ ) indicate that these effects are associated with different propagation modes. This natural decomposition of the wave fields is consistent with Pride's theory (1994): the two wave propagation modes most likely correspond to longitudinal (or extensional modes) and to transverse modes.

The detailed interpretation of the seismo-electromagnetic waveforms is difficult because of the cylindrical geometry and finite length of the column which generate complex propagation modes in the sample. Further investigations relying on numerical simulations are needed to analyze the observed seismo-electric and seismo-magnetic conversions.

## 4 Conclusion

The design of an experimental apparatus within the Low Noise Underground Laboratory allowed us to detect transient seismo-electric and seismo-magnetic signals in a fluid-filled sand column. Their electrokinetic origin has been verified by comparing records in dry and fluid-filled sand. In particular, our measurement protocol ensures that the transient magnetic fields are not due to spurious mechanical vibration of the magnetometers.

The first arrival times of seismo-electric and seismo-magnetic fields clearly indicate that these two fields are coupled to different propagation modes, an observation that is consistent with Pride's (1994) theory. Fast longitudinal modes generate only seismo-electric field whereas transverse modes are coupled to magnetic fields.

Although rather weak, seismo-magnetic signals can be detected with sensitive induction magnetometers but would be difficult to measure outside of the ultra shielded chamber. Nevertheless, transverse modes could be enhanced by considering a horizontal seismic excitation that would generate stronger seismo-magnetic amplitudes. Our results emphasize the complementary nature of seismo-electric and seismo-magnetic measurements to estimate the properties of porous media especially in boreholes.

## 5 Acknowledgements

This research was supported by "ACI Eau et Environnement" of the French Ministry of Research. We are grateful to G. Waysand and S. Gaffet for helpful discussions and authorization to perform this experiment in the LSBB laboratory. We thank M. Auguste, D. Boyer, A. Cavaillou, G. Clerc, R. Guiguet and Y. Orengo for their technical help.

## References

- Ageeva, O. A., B. S. Svetov, G. K. Sherman, and V. Shipulin (1999), E-effect in rocks., *Russian Geology and Geophysics*, 64, 1349–1356.
- Biot, M. A. (1956), Theory of propagation of elastic waves in a fluid-saturated porous solid: I. low frequency range, *J. Acoust. Soc. Am.*, 28(2), 168–178.
- Frenkel, J. (1944), On the theory of seismic and electroseismic phenomena in a moist soil., *J. Phys.*, 8(4), 230–241.
- Gaffet, S., et al. (2003), Simultaneous seismic and magnetic measurements in the low-noise underground laboratory (lsbb) of rustrel, france, during the 2001 january 26 indian earthquake, *Geophys. J. Int.*, 155, 981–990.
- Garambois, S., and M. Dietrich (2001), Seismoelectric wave conversions in porous media: Field measurements and transfer function analysis., *Geophysics*, 66, 1417–1430.
- Garambois, S., and M. Dietrich (2002), Full waveform numerical simulations of seismoelectromagnetic wave conversions in fluid-saturated stratified porous media., *J. Geophys. Res.*, 107(B7).
- Guichet, X., L. Jouniaux, and J.-P. Pozzi (2003), Streaming potential of a sand column in partial saturation conditions, *J. Geophys. Res.*, 108(B3).
- Haartsen, M. W., and S. Pride (1997), Electro seismic waves from point sources in layered media., *J. Geophys. Res.*, 102, 24,745–24,769.

- Ivanov, A. G. (1940), Seismic-electric effect of second kind, *Izv. Akad. Nauk. SSSR, Geog. Geophys.*, 5, 699–726.
- Knight, R., and R. Nolen-Hoeksema (1990), A laboratory study of the dependence of elastic wave velocities on pore scale fluid distribution, *Geophys. Res. Lett.*, (17), 1529–1532.
- Martner, S. T., and N. R. Sparks (1959), The electroseismic effect, *Geophysics*, 24(2), 297–308.
- Mikhailov, O. V., J. Queen, and M. N. Toksöz (2000), Using borehole electroseismic measurements to detect and characterize fractured (permeable) zones., *Geophysics*, 65, 1098–1112.
- Pride, S. (1994), Governing equations for the coupled electromagnetics and acoustics of porous media, *Physical Review B*, 50, 15,678–15,695.
- Pride, S., and M. W. Haartsen (1996), Electroseismic wave properties, *J. Acoust. Soc. Am.*, 100, 1301–1315.
- Takeuchi, N., N. Chubachi, and K. I. Narita (1997), Observations of earthquake waves by the vertical earth potential difference method, *Physics of the Earth and Planetary Interiors*, 101, 157–161.
- Thompson, A. H., and G. A. Gist (1993), Geophysical applications of electrokinetic conversion, *The Leading Edge*, 12, 1169–1173.
- White, B. S. (2005), Asymptotic theory of electroseismic prospecting, *SIAM J. Appl. Math.*, 65, 1443–1462.
- Zhu, Z., and M. N. Toksöz (2005), Seismoelectric and seismomagnetic measurements in fractured borehole models, *Geophysics*, 70(4), F45–F51.
- Zhu, Z., M. W. Haartsen, and M. N. Toksöz (2000), Experimental studies of seismoelectric conversions in fluid-saturated porous media., *J. Geophys. Res.*, 105, 28,055–28,064.

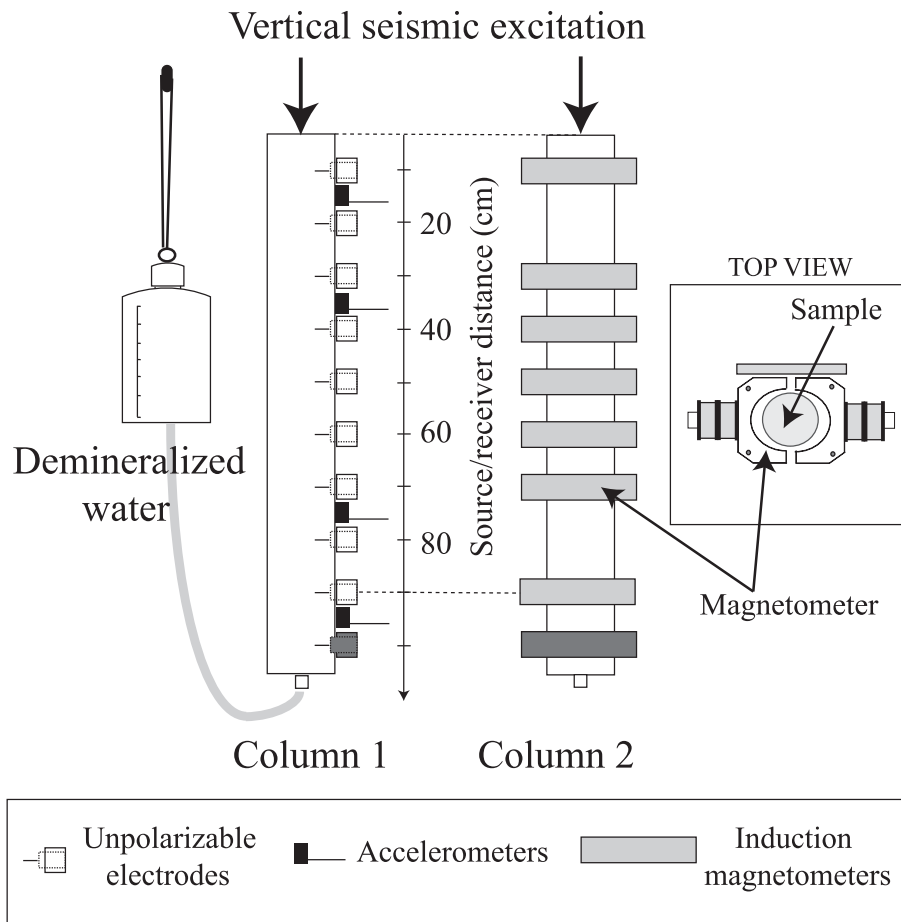


Figure 1: Experimental apparatus for seismo-electric and seismo-magnetic measurements: the column on the left is equipped with 10 unpolarizable electrodes and 4 accelerometers; the column on the right is used for seismo-magnetic measurements only. Magnetometers are fixed on an independent stand to avoid the transmission of disturbing vibrations.

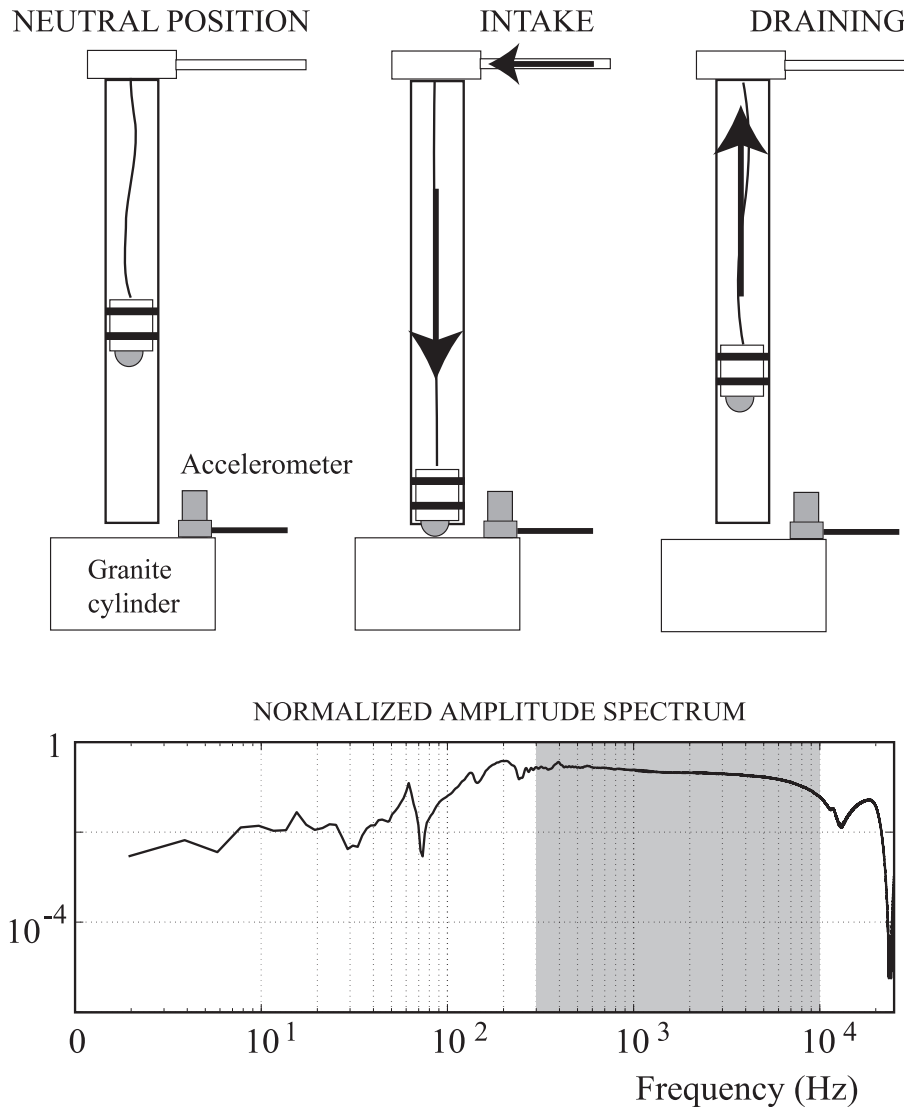


Figure 2: Pneumatic seismic source designed for the seismo-electromagnetic laboratory experiments: a rubis ball (6 mm) is projected with compressed air until it hits a granite cylinder resting on the top part of the sand column. The source time function of the mechanical excitation is measured with a piezo accelerometer on the granite plate intended to record the source time function.

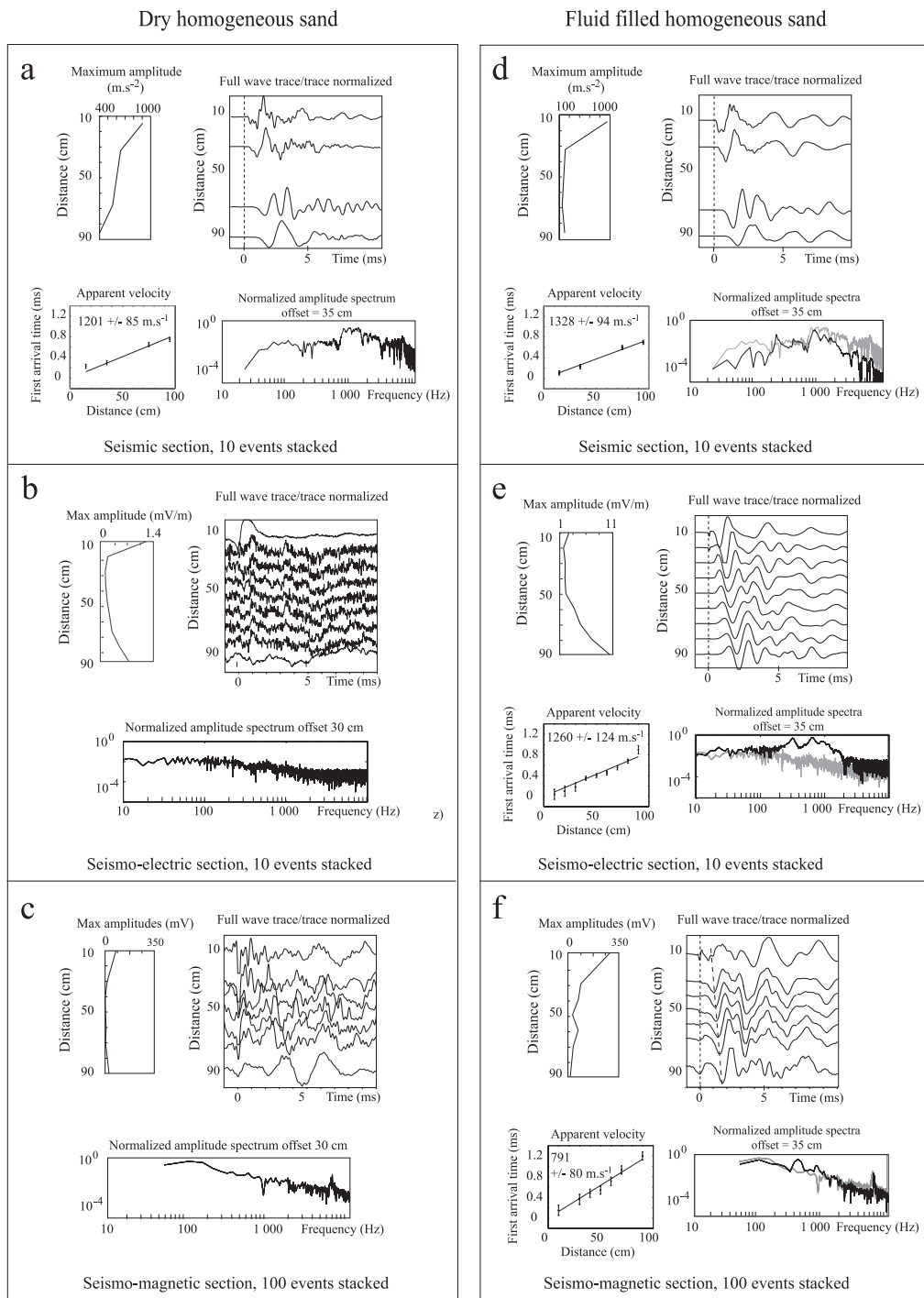


Figure 3: Seismic, seismo-electric and seismo-magnetic signals measured in homogeneous Fontainebleau sand normalized with respect to a  $1000 \text{ m.s}^{-2}$  vertical excitation. Amplitude spectra corresponding to dry conditions are shown in grey in the right-hand side panels for comparison. Apparent velocities have been estimated from the linear regression of first arrivals time.